Assesment of $(Mn,Co)_3 3O_4$ powders for possible coating material for SOFC/SOEC interconnects

To cite this article: D. Szymczewska *et al* 2016 *IOP Conf. Ser.: Mater. Sci. Eng.* **104** 012017

IOP Conf. Series: Materials Science and Engineering **104** (2015) 012017 doi:10.1088/1757-899X/104/1/012017

Assesment of $(Mn,Co)_3O_4$ powders for possible coating material for SOFC/SOEC interconnects

D. Szymczewska[1], S. Molin[2], V. Venkatachalam[2], M. Chen[2], P. Jasinski[1], P.V. Hendriksen[2]

[1] Faculty of Electronics, Telecommunications and Informatics, Gdansk University of Technology, ul. Narutowicza 11/12, 80-233 Gdansk, Poland
[2] Department of Energy Conversion and Storage, Technical University of Denmark, Frederiksborgvej 399, 4000 Roskilde, Denmark

E-mail: author: sebmo@dtu.dk

Abstract. In this work $(Mn,Co)_3O_4$ spinel powders with different Mn:Co ratio (1:1 and 1:2) and from different commercial suppliers are evaluated for possible powder for production of interconnect coatings. Sinterability of the powders is evaluated on pressed pellets sintered in oxidizing and in reducing/oxidizing atmospheres. For selected powder, coatings are then prepared by the electrophoretic deposition method on Crofer 22 APU stainless steel coupons. Effects of dispersant/iodine content and deposition voltage and times are evaluated. Thickness as a function of deposition parameters is described. Results show that with appropriate powder it is possible to produce adherent protective coating with a well-controlled thickness.

1. Introduction

High temperature corrosion of interconnects in Solid Oxide Fuel/Electrolysis stacks is one the most important degradation phenomena for operating stacks [1,2]. Oxides formed on steel interconnects have low electrical conductivity so over time they contribute more and more to the ohmic area specific resistance of the interconnect and thus the full stack [3–5]. Additionally, chromia, formed on the interconnect, can at high pO_2 and in the presence of steam evaporate and poison the oxygen electrode causing more degradation [6–8].

In order to mitigate high temperature corrosion, protective coatings are being developed [9–13]. Coatings can be in general divided into two categories: ones lowering corrosion rates and ones lowering chromia evaporation. For lowering corrosion rates reactive elements (e.g. Y_2O_3, CeO_2) were proven to be very successful whereas for mitigation of chromia evaporation one of the most promising materials reported up to date is the manganese cobalt spinel $(Mn,Co)_3O_4$ (abbreviated as MCO) [14–17]. It offers good electrical conductivity at working temperatures, good thermal expansion coefficient match to the steel and other cell components. Additionally it is very protective towards chromium diffusion – it blocks evaporation of chromia. One of the most important issues for fabrication of a well performing coating is its deposition method and sintering/thermal treatment.

In the available literature several different methods have been reported: electrophoretic deposition [18], physical vapor deposition [19], plasma spraying [20] and other [21–23]. In this work the powders are evaluated for possible use in the electrophoretic deposition [24,25] method developed in our group [26]. Electrophoretic deposition (EPD) technique is quite fragile in terms of powder requirements and

its high quality. Additionally, as the volatility of powders is not certain due to producer's changes, it seems vital to evaluate different available powders to find possibly the best one and its alternatives.

2. Experimental

2.1. MCO powders.

Five different powders produced by four suppliers were tested. Main difference between powders was the Mn:Co elements ratio, as is shown in Table 1. Ratio 1:1 has been purchased from American Elements and Fuel Cell Materials. Ratio 1:2 from Fuel Cell Materials, Marion Technologies and CerPoTech companies. ID of particular powders will be used throughout the text.

Scanning electron microscopy (SEM) pictures and Energy Dispersive X-ray Spectroscopy (EDS) data of the powders were obtained using Hitachi TM3000 with Energy Dispersive X-ray Spectrophotometer Bruker Quantax70. X-ray diffractometry (XRD) measurements of the powders were made using X-ray diffractometer Bruker D8.

Table 1. Studied MCO powders.

Powder source	**Molecular formula**	**Mn:Co ratio**	**ID**
American Elements	$Mn_{1.5}Co_{1.5}O_4$	1:1	AE
Fuel Cell Materials	$Mn_{1.5}Co_{1.5}O_4$	1:1	FCM11
Fuel Cell Materials	$MnCo_2O_4$	1:2	FCM12
Marion Technologies	$MnCo_2O_4$	1:2	MT
CerPoTech	$MnCo_2O_4$	1:2	CPT

2.2. Sinterability.

From AE, FCM11, FCM12 and MT powders pellets were prepared and sintered in four different conditions. Temperatures of 900°C and 1000°C were used. For each temperature two conditions were tested (listed in Table 2). First sintering procedure consisted of only one step – sintering in air. Second procedure had two steps – in the beginning a reducing atmosphere (H_2/N_2) atmosphere was used. After furnace cooling reduced pellets were subjected to sintering in air as a second step. This kind of sintering, first in reducing and then in oxidizing atmosphere is often used for the spinel powder and is termed "redox" sintering.

Table 2. Sintering conditions.

Temperature [°C]	**Cooling/heating rate [°C/h]**	**Sintering time [h]**	**Atmosphere**
900	120	2	Air
1000	120	2	Air
900	120	2	H_2/N_2
	120	2	Air
1000	120	2	H_2/N_2
	120	2	Air

Sintered pellets were measured geometrically to calculate shrinkage and the density of each pellet. Information about density was received also from Archimedes measurements. SEM and EDX

examinations of pellets polished cross-sections were made using Hitachi TM3000 with Energy Dispersive X-ray Spectrophotometer Quantax70.

2.3. Electrophoretic deposition of American Elements powder.

For EPD only American Elements powder was used. For substrates for the deposition, stainless steel coupons were prepared. These were cut from a 0.3 mm thick Crofer 22 APU steel sheet and were subsequently cleaned in ethanol. For the deposition, ethanol and isopropanol in volume ratio 1:1 were mixed as solvents for each suspensions. Three different suspensions were made with varying I_2 content. I_2 amount was different in each suspension: 0.1 wt.%, 0.2 wt.% and 0.3 wt.% of I_2 was used (wt.% in relation to powder weight). Powder content in the suspension was 2 wt.%. Influence of deposition time on layer thickness was checked. Layers were deposited for 1 min, 1.5 min and 2 min. A voltage of 60 V was used for deposition of this set. Additionally, the influence of the voltage during the deposition was also examinated. For this purpose solution with 0.2 wt.% I_2 was used and 2 min deposition time was chosen. Deposition voltages of 30 V, 40 V, 60 V, 80 V and 120 V were evaluated.

Deposited layers were sintered in two steps (redox sintering): 900°C in H_2/N_2 atmosphere for 2 hours, and after furnace cooling again at 900°C for 2 hours in air. Sintered layers were examined using Hitachi TM3000 with Energy Dispersive X-ray Spectrophotometer Quantax70. XRD measurements were made using X-ray diffractometer Bruker D8.

3. Results

In the first step the powder morphology and composition was checked by means of SEM and EDS analysis. This was done in order to ensure powder composition and quality.

SEM analysis of loose powder (attached to a carbon tape) is presented in Figure 1. All powders have fine, less than 1 micrometer grains. Powders produced by CerPoTech, coming from a spray drying process have a core-shell structure and to be suitable for the electrophoretic deposition would require an additional grinding/milling step. Therefore this powder has been excluded from further (sintering) analyses.

As provided by the manufacturers, Mn:Co ratio in the powders should be either 1:1 or 1:2 depending on the composition. All tested powders roughly fall in the expected range with a small and constant deviation, that all powders are slightly more Co rich then the original ratio. About 5-10 at.% enrichment in Co content is measured for all powders.

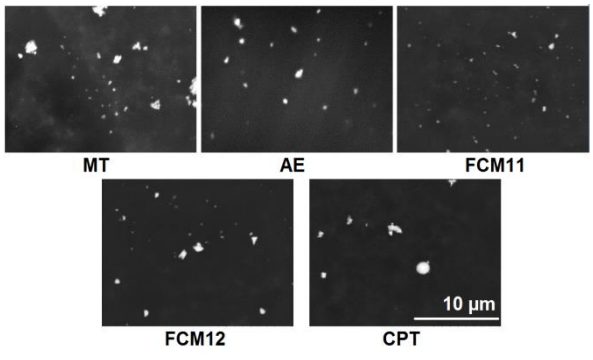

Figure 1. MCO powders

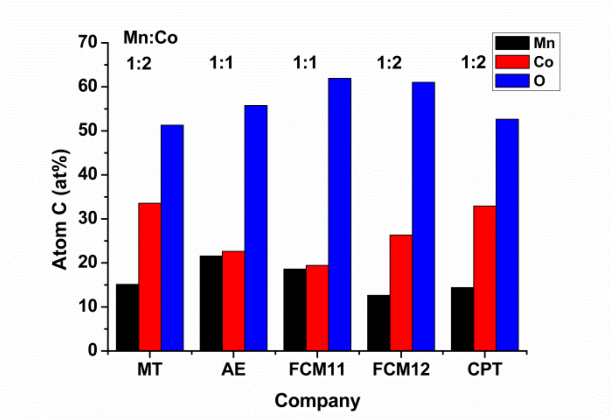

Figure 2. Atomic composition of different as-delivered powders as determined by EDS analysis.

After the SEM/EDS analysis, X-ray diffractometry was performed to check phase purity of the powders. Although no impurities (no foreign elements) were detected by the EDS analysis, still it is

interesting to see phases present. Spinel with a nominal cation ratio of 1:1 is at room temperatures a mixture of a cubic $MnCo_2O_4$ and tetragonal Mn_2CoO_4 phases. This has been confirmed by XRD analysis of powders FCM11 and AE shown in Figure 3. Spectra are quite noisy with broad peaks which might indicate a small crystalline size and/or only partial crystallization of the powders that might require further thermal processing upon heating of the spinel powder, only single cubic phase remain at 800°C. On the other hand, XRD analysis of CPT, FCM12 and MT (Figure 4) powders revealed only a single phase of cubic spinel. In all cases peaks are narrower. No impurity phases were found in any of powders.

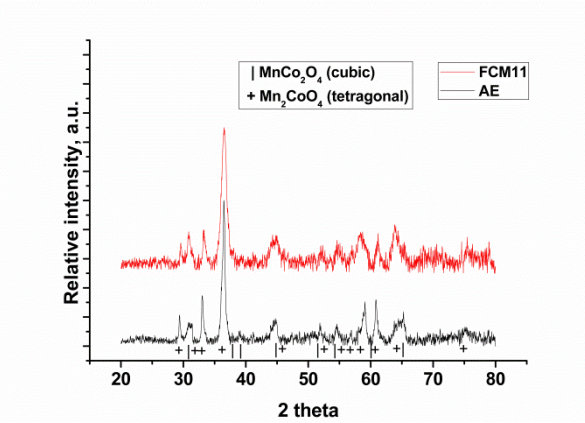

Figure 3. XRD spectra of powders with Mn:Co ratio of 1:1: AE and FCM11.

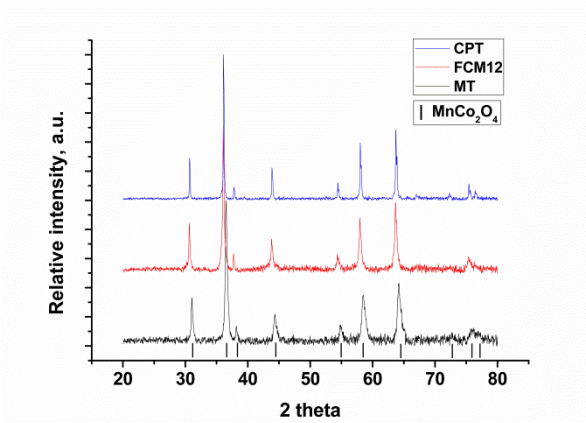

Figure 4. XRD spectra of powders with Mn:Co ratio of 1:2: CPT, MT and FCM12.

3.1. Sinterability

After ensuring powders quality, its sinterability was evaluated. Pellets were pressed from MT, AE, FCM11 and FCM12 powders. Pellets were then sintered in 4 different conditions (two temperatures and two sets of atmospheres). As a measure of sinterability, linear shrinkage, calculated density (based on pellet geometrical shrinkage) and measured density (by Archimedes principle) were used. Linear shrinkage of the pellets is presented in Figure 5. Geometrical measurement can be influenced by several factors: cracks or voids inside, parts of the pellet cracked away etc, so more reliable are the values from the Archimedes measurement and these are presented in Figure 6.

For sintering in air, there is a clear difference between the temperatures of 900°C and 1000°C. MT and AE powders have shown little sintering at 900°C and FCM 11 and FCM12 powders have shown visibly higher shrinkage (~5 %). For sintering at 1000°C, all powders sintered better than at 900°C with shrinkages in the range 5-12 %. Powders FCM11 and FCM12 again have shown superior shrinkage.

Sintering in reducing and then oxidizing atmosphere provided samples with much lower porosities. Even at 900°C samples are less porous then samples sintered in air at 1000°C. After sintering with the redox procedure, density of MT, AE and FCM11 pellets were very similar. Shrinkage was ~25 %. Only pellet prepared from the FCM12 powder reported density and shrinkage lower than expected both for 900°C and 1000°C.

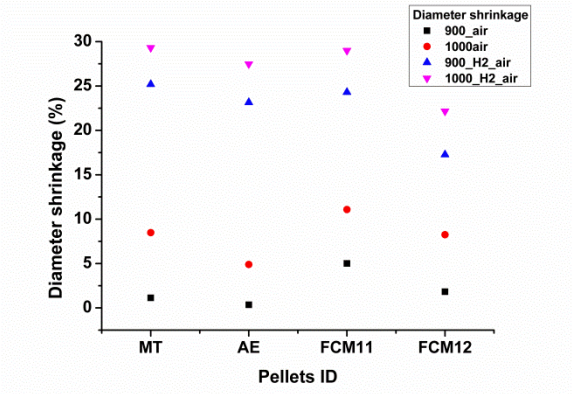

Figure 5. Measured shrinkage of pellets prepared from different powders and sintered at different conditions.

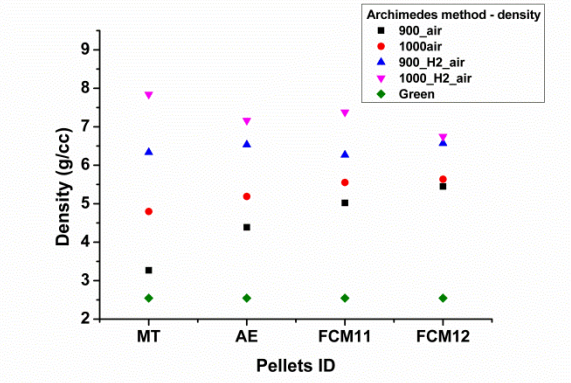

Figure 6. Measured density (by Archimedes method) of pellets prepared from different powders and sintered at different conditions.

Results of shrinkage and density analysis of sintered pellets were further compared with SEM images of pellets cross sections. Cross section images from MT, AE, FCM11 and FCM12 pellets sintered in all 4 conditions are shown in Figure 7. For samples sintered only in air, there is a visible difference in porosities of samples sintered at 900°C and 1000°C. Also grain size increase is noticed, especially from both FCM powders.

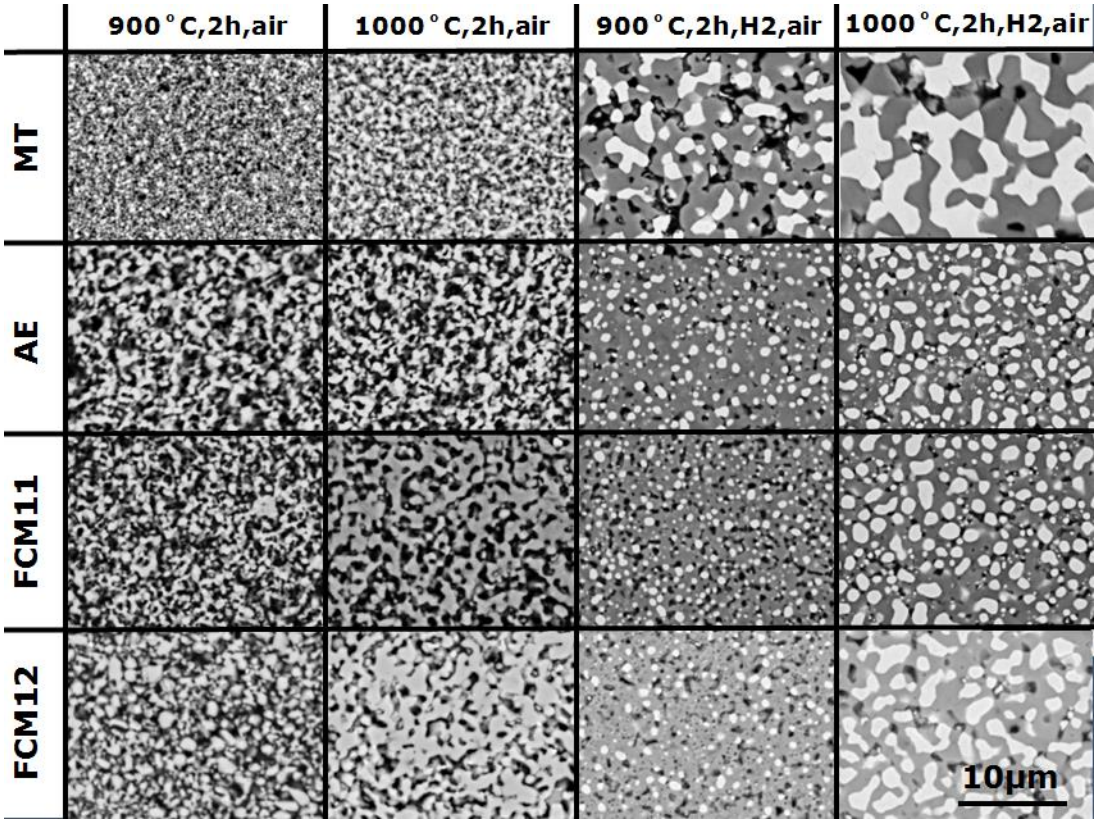

Figure 7. SEM cross sections of polished pellets prepared from different powders and sintered at different conditions.

SEM images of samples sintered using the "redox" procedure show an interesting microstructure consisting of two phases (bright and dark phases). Apparently, the darker phase is the spinel, whereas the brighter phase is a still reduce powder. After sintering in reducing conditions a mix of Co and MnO is formed that upon reoxidation should transform back to the oxide. However, due to kinetic limitations and porous structure of the samples, reoxidation did not occur fast enough. Grain size in MT and FCM12 powders (both powders with a pure cubic phase composition) was higher than for the other two powders with a mixed composition. It seems that at 900°C there is less metallic phase left after oxidation than at 1000°C. This might also indicate that the reduction conditions were not sufficient to fully reduce the powder. To fully oxidize samples longer exposure times would be needed. Due to importance of the sintering step and possible influence of the sintering atmosphere, temperature and time these studies will be continued in the coming future.

3.2. EPD of American Elements powder

3.2.1. Different I_2 contents and deposition time

In order to deposit powders via electrophoretic deposition, particles in the suspension must be given some electric charge. For this purpose in this study I_2 is added to the suspension. Different amount of I_2 has to be added to powders with different surface area etc. For the AE powder amounts of 0.1 wt.%, 0.2 wt.% and 0.3 wt.% were tested. Samples were deposited at 1 min, 1.5 min and 2 min. After deposition coatings were sintered using a "redox" procedure at 900°C. SEM of the as-sintered coatings are shown in Figure 8.

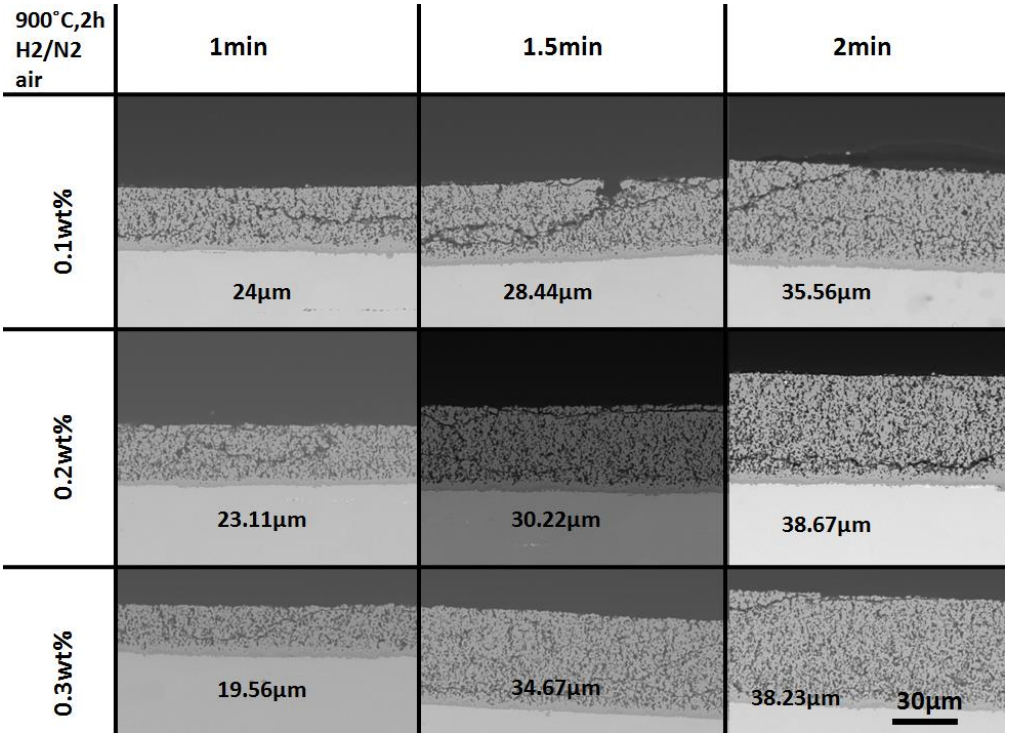

Figure 8. SEM polished cross sections of EPD coatings prepared from AE powder with different iodine content and varying deposition time. Thickness values measured from SEM pictures.

For coatings prepared on steel, there seems to be no unreacted reduced phase present after the oxidation stage of the sintering. It might be due to a relatively low thickness of the coating (~30 µm instead of few mm for pellets) which would facilitate gas exchange due to diffusion.

Thickness of the produced coatings, has been evaluated from the SEM images (Figure 9) and additionally, just after the deposition from the weight gain of sample coupons (Figure 10). For this a 30% porosity was included into calculations. Thickness calculations from the weight gain seems to be representative for real coating thickness and therefore can be used as an assessment of sample quality without the need to destroy the sample.

For the amount of dispersant of 0.1 wt.% and 0.2 wt.% the thickness vs. deposition time is very similar. Whereas for 0.3 wt.% for 1 minute coating thickness is lower than anticipated. One possible reason is that it has been too much of I_2 and some of it reacted at the electrodes and then the amount was reduced and for longer times results were similar for all studied concentrations. It seems from the images, that for higher iodine content, produced coating is less cracked and of higher quality. For 0.3 wt.% of iodine almost no cracks are visible. Looking at the results, using 0.2 wt.% or 0.3 wt.% with the AE powders seems sufficient to ensure homogenous coating.

By controlling the time of deposition coatings with thicknesses ranging from 20 µm to 40 µm might be produced.

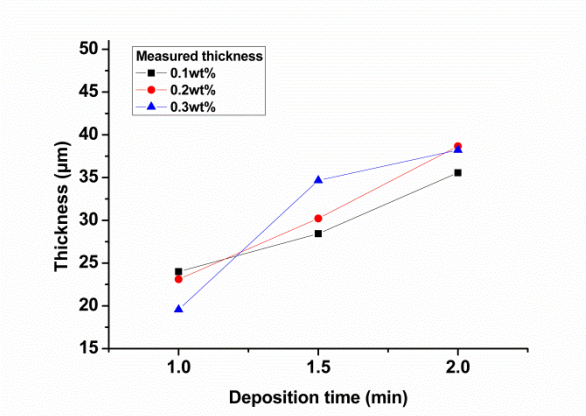

Figure 9. Thickness of the coatings as measured from the SEM cross section images.

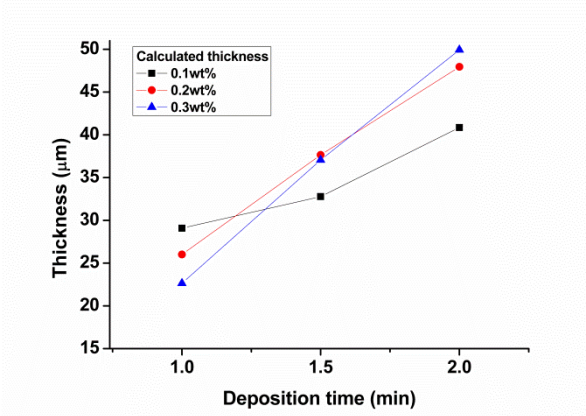

Figure 10. Thickness of the coatings as measured from weight gain after the EPD deposition.

After evaluation of coatings fabrication parameters, cross sections were analysed in more details by SEM/EDS analysis to check chromium diffusion and oxide layer thickness formed on steel during the "redox" sintering procedure. Samples analysed were samples prepared with 0.1, 0.2, 0.3 wt.% iodine and the deposition time was 1 minutes. Results of the analysis are presented in Figure 11. For all samples 3 regions of interest were analysed. "1" is the alloy, analysed just to ensure proper calibration of the EDS. "2" is the interface of the alloy and the coating, where the oxide (Cr_2O_3 and $(Mn,Cr)_3O_4$ spinel should occur). "3" is the bulk of the coating, far away from the interface. The composition of points number "1" is for all samples quite similar and close to the expected composition (between 21 and 24 wt.% as given by the producer of steel). At the interfaces of all samples, Cr rich phase is detected. Due to spatial limitation of the EDS detector it is not possible to clearly distinct the chromium oxide from the bulk of the alloy. Also Mn,Co spinel is detected in point "2". In points "3", major elements present are Mn and Co in the 1:1 ratio as expected for the AE powder. For all samples also Fe and Cr are detected in the coating. Up to 6 wt.% of Cr is present in the coating after sintering. This amount seems quite high. One possibility is that Fe and Cr diffused into the coating during sintering. However, the time was quite short, in total 4 hours at 900°C so maybe metallographic preparation of the samples was not careful enough and some alloy particles were embedded in the coating during polishing. Certainly this will be studied further.

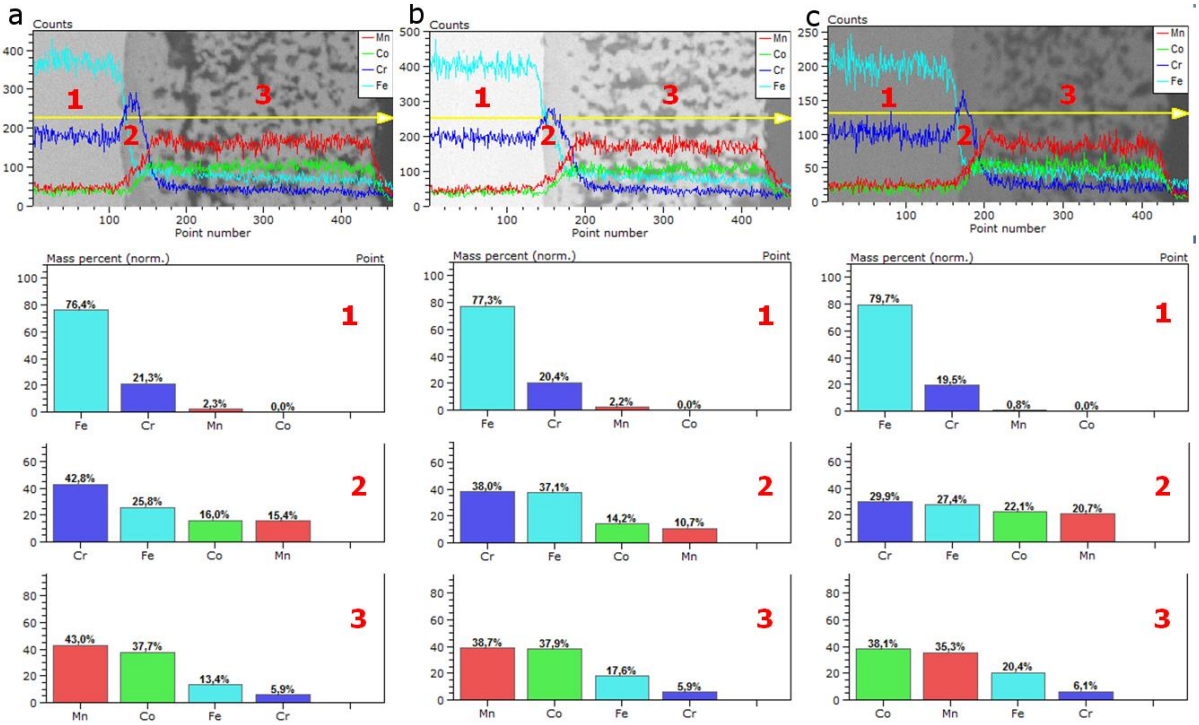

Figure 11. SEM and EDS line profiles of Mn, Co, Cr and Fe on the sintered coatings. Samples with a) 0.1 wt%, b) 0.2wt%, c) 0.3wt% of I_2.

4. Conclusions

In this study several commercial spinel powders were evaluated for their phase purity, composition and sinterability. Four different sintering conditions were used. Results show that sintering using a "redox" procedure results in much denser pellets. For pellets, reduction and/or reoxidation step seems to be kinetically/diffusion limited so that large amount of the reduced phase remain in the pellet after "redox" sintering. This is not present in the coatings prepared on stainless steels.

Electrophoretic deposition method has been evaluated for producing coatings with different dispersant content. For iodine content >0.2 wt.% crack free and homogenous layers were prepared. By finding suitable solvent, dispersant content and deposition parameters (voltage, time) protective coatings for steel interconnects can be produced reproducibly by the EPD method.

5. References

[1] Shaigan N, Qu W, Ivey D G and Chen W 2010 A review of recent progress in coatings, surface modifications and alloy developments for solid oxide fuel cell ferritic stainless steel interconnects *J. Power Sources* **195** 1529–42

[2] Fergus J W J W 2005 Metallic interconnects for solid oxide fuel cells *Mater. Sci. Eng. A* **397** 271–83

[3] Żurek Z, Brylewski T, Jaroń A and Chmura E 2013 Area specific resistance of the scale formed on Crofer 22APU ferritic steel in atmospheres containing SO2 *Solid State Ionics* **234** 33–9

[4] Brylewski T, Nanko M, Maruyama T and Przybylski K 2001 Application of Fe–16Cr ferritic alloy to interconnector for a solid oxide fuel cell *Solid State Ionics* **143** 131–50

[5] Fergus J W 2005 Metallic interconnects for solid oxide fuel cells *Mater. Sci. Eng. A* **397** 271–83

[6] Jiang S P and Chen X 2014 Chromium deposition and poisoning of cathodes of solid oxide fuel cells – A review *Int. J. Hydrogen Energy* **39** 505–31

[7] Wang K, Liu Y and Fergus J W 2011 Interactions Between SOFC Interconnect Coating Materials and Chromia *J. Am. Ceram. Soc.* **94** 4490–5

[8] Gindorf C, Singheiser L and Hilpert K 2005 Vaporisation of chromia in humid air *J. Phys. Chem. Solids* **66** 384–7

[9] Molin S, Chen M and Hendriksen P V 2013 Oxidation study of coated Crofer 22 APU steel in dry oxygen *J. Power Sources* **251** 488–95
[10] Szymczewska D, Molin S, Chen M, Hendriksen P V and Jasinski P 2014 Ceria Based Protective Coatings for Steel Interconnects Prepared by Spray Pyrolysis *Procedia Eng.* **98** 93–100
[11] Molin S, Kusz B, Gazda M and Jasinski P 2008 Protective coatings for stainless steel for SOFC applications *J. Solid State Electrochem.* **13** 1695–700
[12] Yang Z, Walker M S, Singh P, Stevenson J W and Norby T 2004 Oxidation Behavior of Ferritic Stainless Steels under SOFC Interconnect Exposure Conditions *J. Electrochem. Soc.* **151** B669–78
[13] Yang Z, Xia G-G, Li X-H and Stevenson J W 2007 (Mn,Co)3O4 spinel coatings on ferritic stainless steels for SOFC interconnect applications *Int. J. Hydrogen Energy* **32** 3648–54
[14] Larring Y and Norby T 2000 Spinel and Perovskite Functional Layers Between Plansee Metallic Interconnect (Cr-5 wt % Fe-1 wt % Y[sub 2]O[sub 3]) and Ceramic (La[sub 0.85]Sr[sub 0.15])[sub 0.91]MnO[sub 3] Cathode Materials for Solid Oxide Fuel Cells *J. Electrochem. Soc.* **147** 3251–6
[15] Larring Y, Haugsrud R and Norby T 2003 HT Corrosion of a Cr-5 wt % Fe-1 wt % Y[sub 2]O[sub 3] Alloy and Conductivity of the Oxide Scale *J. Electrochem. Soc.* **150** B374–9
[16] Brylewski T, Kucza W, Adamczyk A, Kruk A, Stygar M, Bobruk M and Dąbrowa J 2014 Microstructure and electrical properties of Mn1+xCo2−xO4 (0≤x≤1.5) spinels synthesized using EDTA-gel processes *Ceram. Int.* **40** 13873–82
[17] Liu Y, Kumar C J D and Fergus J W 2012 Electrical Properties of Transition Metal-Doped (Mn,Co) pp 421–7
[18] Smeacetto F, De Miranda A, Cabanas Polo S, Molin S, Boccaccini D, Salvo M and Boccaccini A R 2015 Electrophoretic Deposition of Mn1.5 Co1.5 O4 on Metallic Interconnect and Interaction with Glass-ceramic Sealant for Solid Oxide Fuel Cells Application *J. Power Sources* **280** 379–86
[19] Ajitdoss L C, Smeacetto F, Bindi M, Beretta D, Salvo M and Ferraris M 2013 Mn1.5Co1.5O4 protective coating on Crofer22APU produced by thermal co-evaporation for SOFCs *Mater. Lett.* **95** 82–5
[20] Puranen J, Lagerbom J, Hyvärinen L, Mäntylä T, Levänen E, Kylmälahti M and Vuoristo P 2010 Formation and structure of plasma sprayed manganese-cobalt spinel coatings on preheated metallic interconnector plates *Surf. Coatings Technol.* **205** 1029–33
[21] Malzbender J, Batfalsky P, Vaßen R, Shemet V and Tietz F 2012 Component interactions after long-term operation of an SOFC stack with LSM cathode *J. Power Sources* **201** 196–203
[22] Wei P, Deng X, Bateni M R and Petric A 2007 Oxidation and electrical conductivity Behavior of spinel coatings for metallic interconnects of solid oxide fuel cells *Corrosion* **63** 529–36
[23] Kruk A, Stygar M and Brylewski T 2012 Mn–Co spinel protective–conductive coating on AL453 ferritic stainless steel for IT-SOFC interconnect applications *J. Solid State Electrochem.* **17** 993–1003
[24] Corni I, Ryan M P and Boccaccini A R 2008 Electrophoretic deposition: From traditional ceramics to nanotechnology *J. Eur. Ceram. Soc.* **28** 1353–67
[25] Boccaccini A R and Zhitomirsky I 2002 Application of electrophoretic and electrolytic deposition techniques in ceramics processing *Curr. Opin. Solid State Mater. Sci.* **6** 251–60
[26] Bozza F, Schafbauer W, Meulenberg W A and Bonanos N 2012 Characterization of La0.995Ca0.005NbO4/Ni anode functional layer by electrophoretic deposition in a La0.995Ca0.005NbO4 electrolyte based PCFC *Int. J. Hydrogen Energy* **37** 8027–32

Acknowledgement
Authors would like to thank for the financing: at Gdansk University of Technology by the NCN grant 2012/05/B/ST7/02153 “Functional layers for solid oxide fuel cells“ and at Technical University of Denmark by a grant from the ForskEL project 2015-1-12276 “Towards solid oxide electrolysis plants in 2020” funded by Energinet.dk. D. Sz. wants to acknowledge an internship stipend by the InterPhD programme at GUT.